

## N O T I C E

THIS DOCUMENT HAS BEEN REPRODUCED FROM  
MICROFICHE. ALTHOUGH IT IS RECOGNIZED THAT  
CERTAIN PORTIONS ARE ILLEGIBLE, IT IS BEING RELEASED  
IN THE INTEREST OF MAKING AVAILABLE AS MUCH  
INFORMATION AS POSSIBLE

NASA Technical Memorandum 81392

RADIATION DAMAGE ANNEALING  
MECHANISMS AND POSSIBLE  
LOW TEMPERATURE ANNEALING  
IN SILICON SOLAR CELLS

(NASA-TM-81392) RADIATION DAMAGE ANNEALING  
MECHANISMS AND POSSIBLE LOW TEMPERATURE  
ANNEALING IN SILICON SOLAR CELLS (NASA)  
10 p HC A02/MF A01

N80-15558

CSCL 10A

G3/44    Unclass  
46638

Irving Weinberg and Clifford K. Swartz  
Lewis Research Center  
Cleveland, Ohio

Prepared for the  
Fourteenth Photovoltaic Specialists Conference  
sponsored by the Institute of Electrical and Electronics Engineers  
San Diego, California, January 7-10, 1980

# RADIATION DAMAGE ANNEALING MECHANISMS AND POSSIBLE LOW TEMPERATURE

## ANNEALING IN SILICON SOLAR CELLS

by Irving Weinberg and Clifford K. Swartz

National Aeronautics and Space Administration  
Lewis Research Center  
Cleveland, Ohio 44135

### ABSTRACT

The defect responsible for reverse annealing in 2 ohm-cm  $n^+p$  silicon solar cells has been identified. This defect, with energy level at  $E_v + 0.30$  eV, has been tentatively identified as a boron-oxygen-vacancy complex. Our calculations also suggest that its removal could result in significant annealing for 2 ohm-cm and lower resistivity cells at temperatures as low as 200° C. These results were obtained by use of an expression derived from the Shockley-Read-Hall recombination theory which relates measured diffusion length ratios to relative defect concentrations and electron capture cross sections. The relative defect concentrations and one of the required capture cross sections are obtained from Deep Level Transient Spectroscopy. Four additional capture cross sections are obtained using our diffusion length data and data from temperature-dependent lifetime studies. These calculated results are in reasonable agreement with experimental data. However, since identification of the atomic constitution of the defect at  $E_v + 0.30$  eV is speculative, additional effort is required to effect a firm identification of the sub-microscopic constituents of this harmful defect.

### INTRODUCTION

One barrier to extending mission times in space is the radiation damage suffered by the silicon solar cell power supply. Overcoming this barrier by complete elimination of radiation damage to the cell remains an elusive research goal. A more pragmatic approach is to thermally anneal the radiation damage. Significant recovery of the performance of radiation-damaged silicon solar cells can be effected by annealing at temperatures of about 400° C and above (1). Exact temperatures required and the amount of recovery accomplished depend upon radiation dose level and the silicon type, dopant, and resistivity. However, considerably lower temperatures would be required to avoid irreversible damage to array components while achieving the in-situ annealing required to extend mission lifetimes in space. One approach for achieving lower annealing temperatures lies in identification and removal of the major defect(s) whose effect on cell performance necessitates use of the higher annealing temperatures. The primary objective of the present work is to identify this defect(s). An additional barrier to low tempera-

ture annealing is the reverse annealing phenomena usually observed in silicon solar cells.

The phenomenon of reverse annealing has been observed in bulk silicon (2) and in silicon solar cells (1,3). Since, during reverse anneal, cell performance degrades at temperatures well below 400° C, it constitutes a detriment toward the achievement of annealing at low temperatures. Thus, to achieve low temperature annealing, identification and elimination of the defect or defects responsible for both the reversal and the high-temperature annealing is necessary. In this paper we report efforts to identify the defect whose presence necessitates high annealing temperatures and the defect responsible for the reverse annealing phenomena in silicon solar cells. In the present case, we combine information from Deep Level Transient Spectroscopy (DLTS) (4) with diffusion length measurements and the Shockley-Read-Hall (SRH) recombination theory (5,6) to identify the responsible defects.

### EXPERIMENTAL

Irradiations and isochronal annealing were performed on  $n^+p$  silicon solar cells with 0.1 and 2 ohm-cm boron-doped base resistivities. Starting material for the 2 ohm-cm cell was Czochralski grown while the starting material for the 0.1 ohm-cm cell was vacuum float zone refined single crystal silicon. The cells were irradiated by 1 MeV electrons to a fluence of  $10^{15}$  cm<sup>-2</sup>. After irradiation, the cells were isochronally annealed in 50° C steps, the cells being held at each fixed temperature point for 20 minutes. Minority carrier diffusion lengths and AMO I-V measurements were obtained at room temperature before and after irradiation and after each step in the isochronal anneal. Diffusion lengths were measured by an X-ray excitation technique (7), while the AMO I-V measurements were obtained using a xenon-arc solar simulator.

### RESULTS

Figure 1 shows the percent change in short-circuit current during the isochronal anneal for both the 0.1 and 2 ohm-cm cells. The reverse annealing phenomena occurs at temperatures between about 200° to 350° C for the 2 ohm-cm cell. These data are similar to those reported by others (1).

Although a small tendency toward reverse annealing appears in the 3.1 ohm-cm data at 200°C, the effect is essentially absent, within experimental error, in the low resistivity cells studied here. Figure 2 shows the behavior of the diffusion length ratio  $L_T^2/L_{IRR}^2$  for the same two cells during isochronal anneal. The subscript T denotes a measurement made after isochronal anneal at temperature T while the subscript IRR denotes the room temperature measurement made immediately after irradiation. For reasons which are clarified in the next section, these diffusion length ratios are related to measured defect concentrations and capture cross sections. Thus, to further analyze these data, both defect concentrations and capture cross sections are required. The relative defect concentrations shown in Fig. 3 are obtained from the DLTS results of Ref. 4, normalized to the present fluence of 1015/cm<sup>2</sup>.

#### THEORY AND CALCULATIONS

##### Working Equation

To obtain an equation relating the diffusion length data to defect parameters such as carrier capture cross sections and relative defect concentrations, we use the Shockley-Read-Hall (SRH) theory of recombination (5,6). Our starting point is the SRH expression for  $\tau_i$  the carrier lifetimes due to the *i*th single level defect. For low injection conditions we have;

$$\frac{1}{\tau_i} = \frac{N_i}{\frac{1}{v_p \sigma_{pi}} \left( \frac{n_o + n_i}{n_o + p_o} \right) + \frac{1}{v_n \sigma_{ni}} \left( \frac{p_o + p_i}{n_o + p_o} \right)} \quad (1)$$

Where  $N_i$  is the concentration of the *i*th defect,  $n_o$  and  $p_o$  are equilibrium electron and hole concentrations,  $v_n$  and  $v_p$  are thermal velocities for electrons and holes,  $\sigma_{pi}$  and  $\sigma_{ni}$  are hole and electron capture cross sections for the *i*th defect and  $n_i$  and  $p_i$  are calculated from the relations:

$$n_i = N_c \exp \left( \frac{E_i - E_c}{kT} \right) \quad (2a)$$

$$p_i = N_v \exp \left( \frac{E_v - E_i}{kT} \right) \quad (2b)$$

$N_c$  and  $N_v$  are the density of states for the conduction and valence bands  $k$  is the Boltzmann constant and  $E_i$  is the energy level of the *i*th defect. The thermal velocities are obtained from the relations:

$$v_p = \left( \frac{3kT}{m_h} \right)^{1/2} \quad (3a)$$

$$v_n = \left( \frac{3kT}{m_e} \right)^{1/2} \quad (3b)$$

where  $m_h$  and  $m_e$  are hole and electron effective masses, respectively.

For P type silicon  $p_o$  is measured and  $n_o$  calculated from the relation:

$$n_o p_o = n_i^2 \quad (4)$$

where  $n_i$  is the intrinsic carrier concentration.

Using Eqs. (2), (3), and (4), we find for the defects in Fig. 3 that:

$$\frac{p_o + p_i}{n_o + p_o} \approx 1$$

$$\frac{n_o + n_i}{n_o + p_o} \ll 1$$

and

$$v_n \approx v_p \approx 2 \times 10^7 \text{ cm/sec}$$

Hence Eq. (1) simplifies to

$$\frac{1}{\tau_i} \approx N_i \sigma_{ni} v_n = N_{\max} R_i \sigma_{ni} v_n \quad (5)$$

where  $R_i$  is the relative concentration of the *i*th defect with

$$R_i = \frac{N_i}{N_{\max}} \quad (6)$$

$N_{\max}$  being the maximum defect concentration measured by DLTS during the isochronal anneal. For example in Fig. 3,  $N_{\max}$  is obtained from the peak amplitude of the  $E_v + 0.38 \text{ eV}$  defect (4)

Since

$$\frac{L_T^{-2}}{L_{IRR}^{-2}} = \frac{\frac{1}{\tau} T}{\frac{1}{\tau_{IRR}}} = \frac{\left( \sum_i \frac{1}{\tau_i} \right) T}{\left( \sum_i \frac{1}{\tau_i} \right)_{IRR}} \quad (7)$$

We obtain the required relation

$$\frac{L_T^{-2}}{L_{IRR}^{-2}} \approx \frac{\left( \sum_i R_i \sigma_{ni} \right) T}{\left( \sum_i R_i \sigma_{ni} \right)_{IRR}} \quad (8)$$

### Capture Cross Sections

The capture cross sections obtained from DLTS (4), are listed in Table I. Since the electron capture cross section,  $\sigma_n$ , for only one defect ( $E_c - 0.2$  eV) is available from DLTS, we cannot calculate diffusion length ratios from Eq. (8) using only this DLTS result. We have therefore obtained the necessary additional  $\sigma_n$  values by other methods.

With respect to the defects at  $E_v + 0.38$  eV and  $E_v + 0.23$  eV, temperature dependent lifetime studies in 1.5 ohm-cm p-type silicon yield values for the ratio  $\sigma_n/\sigma_p$  from which  $\sigma_n$  is calculated (8). From Ref. 8, for the  $E_v + 0.38$  eV defect  $\sigma_n/\sigma_p \approx 150$  and for the defect at  $E_v + 0.23$  eV,  $\sigma_n/\sigma_p \approx 1300$  from which the  $\sigma_n$  values for these defects shown in Table II are calculated. For the remaining defects, values for  $\sigma_n$  were computed by fitting Eq. (8) to the diffusion length data of Fig. 2 at 250° and 300° C using  $R_L$  values from Fig. 3. In this way, the electron capture cross sections for the defects at  $E_v + 0.30$  eV and  $E_v + 0.26$  eV were obtained. Thus, the required cross sections for all but the defect at  $E_v + 0.20$  eV are obtained for use in Eq. (8). Since we cannot evaluate  $\sigma_n$  for this latter defect, it is assumed that this defect can be ignored in subsequent calculations.

### Calculations

Diffusion length ratios calculated from Eq. (8) using the cross sections of Table II and the data of Fig. 3 are shown in Fig. 4 for the 2 ohm-cm cell. The solid curve in Fig. 4 is the curve drawn through the measured diffusion length ratios shown in Fig. 2. The measured and calculated values are in reasonable agreement. The assumption that  $E_v + 0.2$  eV center could be ignored appears warranted. Omitting the defect at  $E_v + 0.30$  eV and repeating the calculations, we find that the reverse annealing disappears from the calculated results as shown in Fig. 5. We note that of the five defects considered in these calculations, only this latter defect eliminates the reverse annealing phenomena when omitted from the calculations. Hence, we conclude that the defect at  $E_v + 0.30$  eV is responsible for the reverse annealing observed in the present 2 ohm-cm cells. These calculations also suggest that removal of the defect at  $E_v + 0.3$  eV could result in significant cell recovery or annealing at 200° C (Fig. 5).

In addition to the 2 ohm-cm cell, Ref. 4 reports the relative defect concentration for a 0.3 ohm-cm cell shown in Fig. 6. These data were used to calculate diffusion length ratios using the capture cross sections of Table II and Eq. (8). We are unable to obtain a capture cross section for the defect at  $E_v + 0.48$  eV, hence it is omitted from the calculation. The calculated results for the low resistivity cell are shown in Fig. 7. These results predict the absence of reverse annealing in this low resistivity cell and are in qualitative agreement with our data for the 0.1 ohm-cm cell. The omission of the center at  $E_v + 0.48$  eV seems warranted. Repeating the calculation by omitting the defect at  $E_v + 0.30$  eV

yields the dotted line of Fig. 7. These results suggest that removal of the defect at  $E_v + 0.30$  eV could also result in significant cell recovery or annealing at 200° C. In this respect it is significant to note that cells of this low resistivity presently require annealing temperatures higher than 400° C to effect such recovery.

### DISCUSSION

The preceding indicates that the defect at  $E_v + 0.30$  eV is responsible for the observed reverse annealing in the 2 ohm-cm cell. The calculations also suggest that the same defect is responsible for the required high annealing temperatures and that its removal could result in significant performance annealing at 200° C. In making this suggestion, it is implied that with removal of the responsible defect, another will not take its place. The present work is incomplete in the sense that detailed consideration has not been given to this possibility. Before a scheme can be devised to eliminate the  $E_v + 0.3$  eV defect, we must identify its atomic composition. It is therefore important to speculate on the nature of this defect. It is reported that the  $E_v + 0.30$  eV defect always appears when the  $E_c - 0.27$  eV defect disappears (4). The two defects are related in the sense that the  $E_c - 0.27$  eV defect can be called the parent to the defect at  $E_v + 0.30$  eV. Hence, the atomic constitution of both defects is of importance.

The defect at  $E_v + 0.30$  eV has been tentatively identified as a boron-oxygen-vacancy complex (4). The  $E_c - 0.27$  eV defect increases in concentration with increasing boron concentration and has been identified as a boron interstitial-oxygen interstitial complex (4). An alternate identification asserts that the  $E_c - 0.27$  eV defect is composed of a boron interstitial-boron substitutional pair (9). Both a firmer identification of the  $E_v + 0.30$  eV defect and additional research directed at choosing between competing identifications for the  $E_c - 0.27$  eV parent defect are required. Such identifications would be an invaluable guide to processing efforts aimed at decreasing the concentration of these radiation induced defects.

### SUMMARY AND CONCLUSION

We have used the Shockley-Read-Hall recombination theory to obtain an expression relating measured diffusion length ratios to defect concentrations and electron capture cross sections in p-type silicon. Because only one of the many required cross sections was available from DLTS data, we utilized temperature dependent lifetime studies and the measured diffusion length data to determine four additional electron capture cross sections. Calculations using these cross sections and reported relative defect concentrations show reasonable agreement between calculated and measured diffusion length ratios. Our calculated results indicate that a defect at  $E_v + 0.30$  eV is responsible for the reverse annealing observed in 2 ohm-cm  $n^+/p$  silicon solar cells. It was also determined by calculation that removal of this same defect could result in significant annealing at temperatures as

low as 200° C for 2 ohm-cm and lower resistivity cells. Hence, we identify the defect, whose energy level is at  $E_v + 0.30$  eV, as the major defect whose effect on cell performance necessitates use of annealing temperatures around 400° C. Since a firm identification of its atomic constituents has not been made, additional identification efforts are required in order to guide processing efforts directed at removal of the harmful defect.

#### REFERENCES

1. P. H. Fang, "Thermal Annealing of Radiation Damage in Solar Cells," NASA TM X-55399, Nov. 1965.
2. R. R. Hasiguti and S. Ishino, "Defect Mobility and Annealing in Irradiated Germanium and Silicon," in Radiation Damage in Semiconductors, M. Hulin, Ed., New York: Academic Press, 1964, pp. 259-273.
3. P. H. Fang and Y. M. Liu, "Temperature Dependence of Radiation Damage in Silicon," Phys. Lett., vol. 20, pp. 344-346, 1966.
4. P. M. Mooney, L. J. Cheng, M. Suli, J. D. Gerson, and J. W. Corbett, "Defect Energy Levels in Boron-Doped Silicon Irradiated with 1-MeV Electrons," Phys. Rev. B, vol. 15, pp. 3836-3843, 1977.
5. R. N. Hall, "Electron-Hole Recombination in Germanium," Phys. Rev., vol. 87, p. 387, 1952.
6. W. Shockley and W. T., Jr., Read, "Statistics of the Recombination of Holes and Electrons," Phys. Rev., vol. 87, pp. 835-842, 1952.
7. W. Rosenzweig, "Diffusion Length Measurements by Means of Ionizing Radiation," Bell Syst. Tech. J., vol. 41, pp. 1573-1588, 1962.
8. J. R. Srour, O. L., Jr., Curtis, S. Othmer, K. Y. Chiu, and V. D. Doekar, "Radiation Effects on Semiconductor Materials and Devices," HDL-TR-171-4, Northrop Corp., Hawthorne, Cal., p. 126, 1973. (AD-776420)
9. L. C. Kimerling, "Defect States in Electron-Bombarded Silicon," in International Conference on Radiation Effects in Semiconductors, Dubrovnik, Yugoslavia, 6-9 Sept. 1976, N. B. Urii and J. W. Corbett, Eds., London: Institute of Physics, 1977, pp. 221-23.

TABLE I. - CAPTURE CROSS SECTIONS FROM DLTS

Defect energy level, eV	Capture cross sections, cm <sup>2</sup>	
	$\sigma_p$	$\sigma_n$
$E_v + 0.38$	$2 \times 10^{-16}$	-----
$E_c - 0.27$	-----	$2 \times 10^{-13}$
$E_v + 0.23$	$3 \times 10^{-16}$	-----
$E_v + 0.30$	$2 \times 10^{-16}$	-----
$E_v + 0.26$	-----	-----
$E_v + 0.2$	-----	-----

TABLE II. - ELECTRON CAPTURE CROSS SECTIONS

Energy level of defect, eV	Electron capture cross section, cm <sup>2</sup>	Method for obtaining section
$E_c - 0.27$	$2 \times 10^{-13}$	DLTS
$E_v + 0.38$	$3 \times 10^{-14}$	$\sigma_n / \sigma_p \approx 150^*$
$E_v + 0.23$	$3.9 \times 10^{-13}$	$\sigma_n / \sigma_p \approx 1300^*$
$E_v + 0.30$	$3.6 \times 10^{-13}$	Fit of $1/L^2$ ratio to DLTS (250° C)
$E_v + 0.26$	$9.5 \times 10^{-14}$	Fit of $1/L^2$ ratio to DLTS (300° C)

\* Computed from  $\sigma_n / \sigma_p$  ratios for 1.5 ohm-cm p-type (FZ) from Srour, Curtis, Othmer, Chiu, and Doekar: Report HDL-TR-171-4.

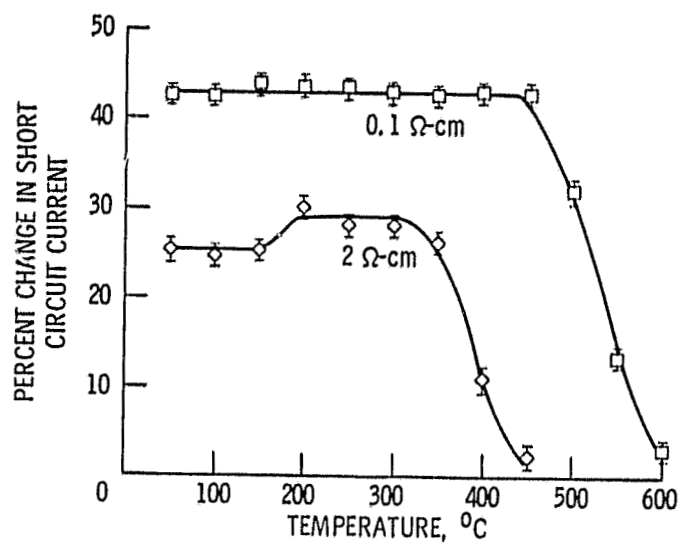


Figure 1. - Isochronal anneal of  $n^+p$  silicon solar cells after 1 MeV electron. Irradiation:  $\phi = 10^{15}/\text{cm}^2$ . (Time at temperature, 20 min.)

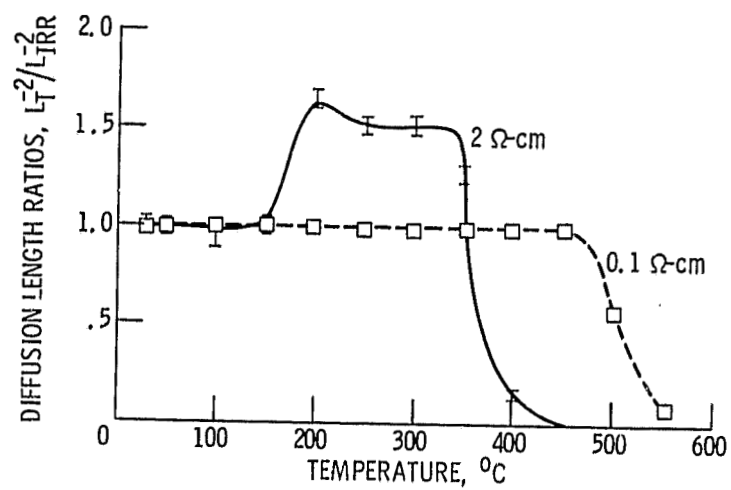


Figure 2. - Measured diffusion length ratios during isochronal anneal.

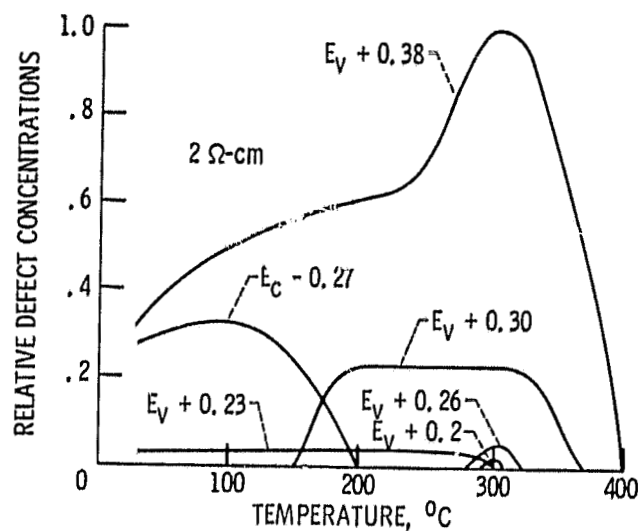


Figure 3. - Relative defect concentrations from DLTS (after Mooney et al.).

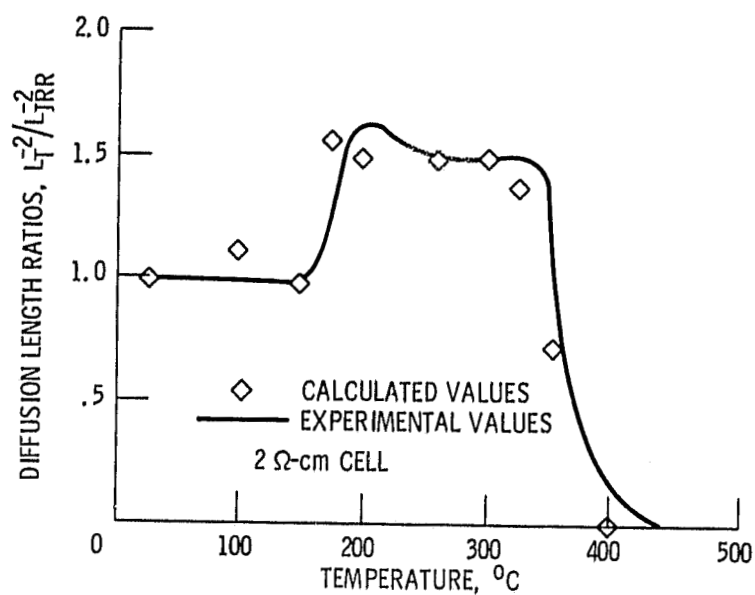


Figure 4. - Comparison of calculated and measured diffusion length ratios.



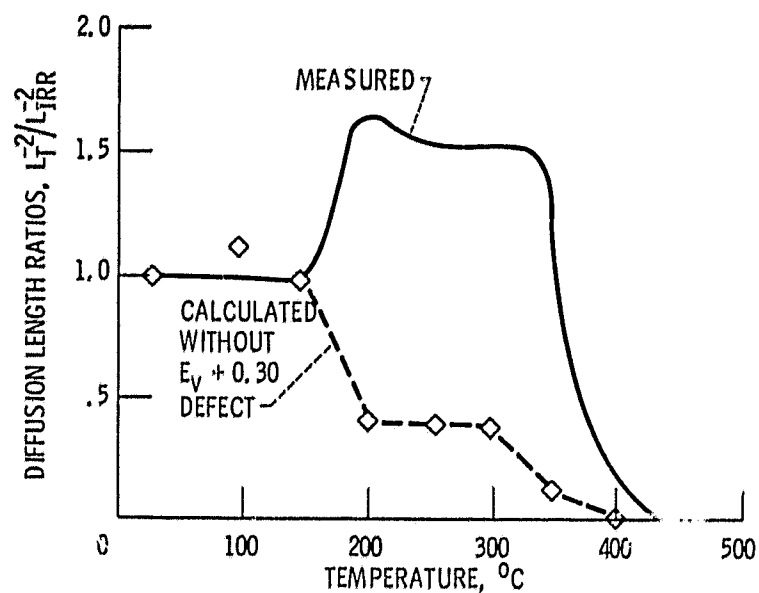


Figure 5. - Calculated and measured diffusion length ratios omitting the  $E_V + 0.30$  defect.

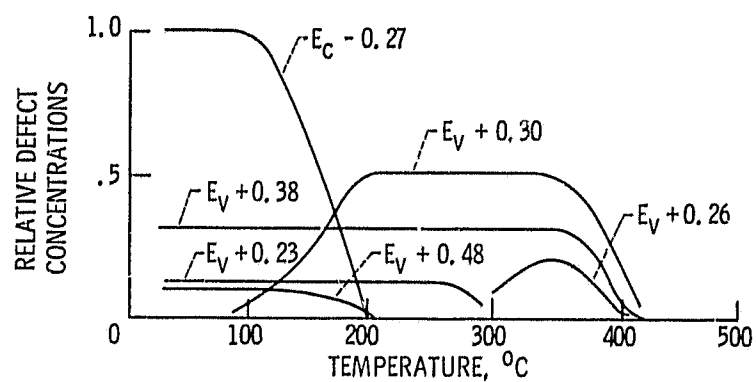


Figure 6. - DLTS data for 0.3  $\Omega\text{-cm}$  P-Si. Isochronally annealed after 1 MeV electron irradiation (after Mooney et al.).

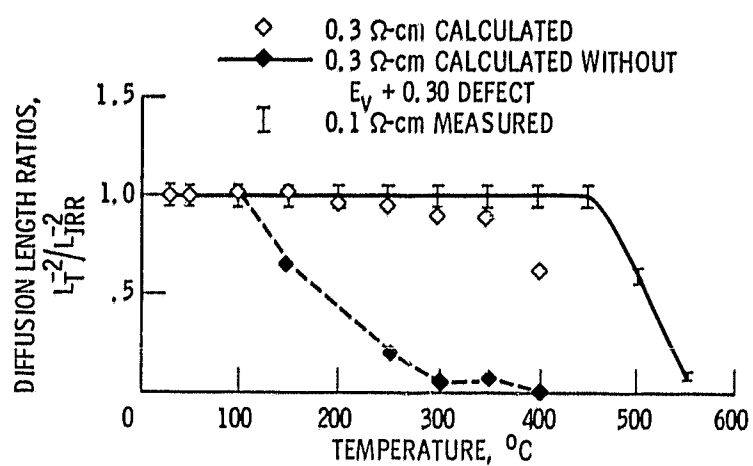


Figure 7. - Calculated and measured diffusion length ratios, low resistivity P-Si.

1 Report No NASA TM-81392		2 Government Accession No		3 Report's Catalog No	
4 Title and Subtitle RADIATION DAMAGE ANNEALING MECHANISMS AND POSSIBLE LOW TEMPERATURE ANNEALING IN SILICON SOLAR CELLS				5 Report Date	
7 Author(s) Irving Weinberg and Clifford K. Swartz				6 Performing Organization Date	
9 Performing Organization Name and Address National Aeronautics and Space Administration Lewis Research Center Cleveland, Ohio 44135				8 Performing Organization Report No E-302	
12 Sponsoring Agency Name and Address National Aeronautics and Space Administration Washington, D.C. 20546				10 Work Unit No	
				11 Contract or Grant No	
				13 Type of Report and Period Covered Technical Memorandum	
				14 Sponsoring Agency Code	
15 Supplementary Notes					
16 Abstract The defect responsible for reverse annealing in 2 ohm-cm $n^+/p$ silicon solar cells has been identified. This defect, with energy level at $E_v + 0.30$ eV, has been tentatively identified as a boron-oxygen-vacancy complex. Our calculations also suggest that its removal could result in significant annealing for 2 ohm-cm and lower resistivity cells at temperatures as low as 200° C. These results were obtained by use of an expression derived from the Shockley-Read-Hall recombination theory which relates measured diffusion length ratios to relative defect concentrations and electron capture cross sections. The relative defect concentrations and one of the required capture cross sections are obtained from Deep Level Transient Spectroscopy. Four additional capture cross sections are obtained using our diffusion length data and data from temperature dependent lifetime studies. These calculated results are in reasonable agreement with experimental data. However, since identification of the atomic constitution of the defect at $E_v + 0.30$ eV is speculative, additional effort is required to effect a firm identification of the sub-microscopic constituents of this harmful defect.					
17. Key Words (Suggested by Author(s)) Radiation damage Temperature annealing Reverse annealing			18. Distribution Statement Unclassified - unlimited STAR Category 44		
19. Security Classif. (of this report) Unclassified		20. Security Classif. (of this page) Unclassified		21. No. of Pages	
				22. Price*	

\* For sale by the National Technical Information Service, Springfield, Virginia 22161